RF Profile and Off-Resonance Effects on the Measured RF Field Map

J. Wang[1], M. Qiu[1], W. Mao[2], M. B. Smith[2], R. T. Constable[1,3]

[1]Department of Diagnostic Radiology, Yale University, New Haven, CT, United States, [2]Department of Radiology, The Pennsylvania State University College of Medicine, Hershey, PA, United States, [3]Department of Biomedical Engineering, Yale University, New Haven, CT, United States

ABSTRACT

An assessment of the transmit field for different RF pulses (sinc, Gaussian and truncated sinc RF pulses) and off-resonance frequencies is shown. The influence of these factors on the measured transmission field maps among different RF types is significant with variations above 20%. Off-resonance frequencies have little impact on the absolute value of the averaged transmission field map, but can significantly alter the distribution of the field map measured. Thus, measured RF field maps include contributions from both the RF pulse profile and off-resonance effects.

INTRODUCTION

Because of the potential advantages in SNR, T2*, contrast, spatial resolution, and imaging time, the static magnetic field strength for human imaging has been pushed to 9.4 T and higher. The images acquired at high field in humans exhibit large signal distribution variations from non-tissue characteristics and these variations can strongly impair the quality of the data obtained at high field. Directly measuring the transmit field map allows for correction of the signal intensity nonuniformities that result, and thus it is important to be able estimate such maps *in vivo*. The measured transmit field includes not only the contributions of wave behavior and RF penetration, but also the contributions of other RF issues. Here, the effects of different RF pulses and off-resonance frequencies on the transmit field map are studied.

THEORY

For a spin echo (SE) sequence with excitation flip angle α and refocusing flip angle 2α, the transmission field for non-interacting spins without transverse coherence, can be written as [1]: $B_1^+ = \frac{1}{\gamma\tau}\cdot\arccos\left(\lambda/8\right)^{1/3}$ where γ is the magneto-gyric ratio, λ is the ratio of signal intensities of two spin echo images which are acquired with different excitation flip angles of α and 2α while maintaining the other imaging parameters (TE, TR) fixed. τ is the duration of the RF pulse, and B_1^+ is a positive circularly polarized component of the RF field, which rotates in the same direction as nuclear spin precession.

METHOD

Numerical simulations for the transmit field and reception sensitivity were performed with the XFDTD program (REMCOM, Inc., State College, PA 16805), which uses a Finite Difference Time Domain method to solve Maxwell's wave equations [2, 3]. The two spheres phantoms with the diameter of 18 and 6 cm were simulated with different conductivity (0.34 and 1.634 Ω.m) and relative permittivities (5.9 and 68.19), respectively. Phantom and in vivo brain images were acquired on a Siemens 3.0 T Trio system. The transmission field maps of both the phantom and in vivo images were estimated using two images obtained with segmented spin echo-EPI (excitation flip angles of 60^o and120^o and refocusing flip angles of 120^o and 240^o, matrix 128^2) with different RF excitation pulses (sinc, Gaussian and truncated sinc pulses). Off-resonance frequencies ranging from 0 Hz to 150 Hz were also considered.

RESULTS AND DISCUSSION

Fig. 1 shows simulation results for the field map B_1, transmit field B_1^+ and reception sensitivity B_1^- at the 20 MHz (Fig. **1a-c** at 0.5 T) and 128 MHz (Fig. 1**e-f** at 3.0 T). At 0.5 T, quasi-static field theory is good approximation for depicting the RF field and the interaction between RF and objects and it is apparent that the small sphere does not give rise to significant field change at low frequency. The B_1, B_1^+ and B_1^- have almost identical distributions and can be used interchangeably (Fig. **1a-c**). At 3.0 T, the differences between B_1, B_1^+, and B_1^- become pronounced around the small sphere, shown in Fig. **1d-f**. The RF transmit field map can be estimated using Eq. [1]. Fig. **2** displays the measured transmit field maps for different RF pulses (Fig. **2a-c**) and their calibration factors (Fig. **2d**). The calibration factors change with pulse types. The difference of the measured field maps across the three RF pulses can be significant ranging up to 20%. Off-resonance effects also give rise to changes in the field distribution. The difference in the measured field maps between the off-resonance and on-resonance conditions, increases with the increasing shift off-resonance, however these effects are small. With off-resonance frequencies up to 120 Hz, the maximum difference of the measured field maps is of the order of 3%, which may be important for precise quantitative work.

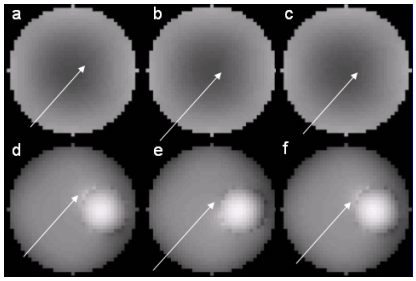

Fig. 1 Distributions of the magnitudes of the RF field (B_1) and the counter-clockwise (B_1^+) and clockwise (B_1^-) rotating components of B_1 at 20 MHz and 128 MHz .

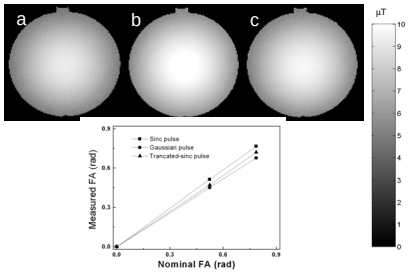

Fig. 2 the measured field map for sinc (**a**), Gaussian (**b**), truncated sinc (**c**) and their RF calibration factors

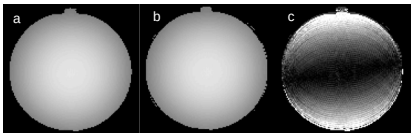

Fig 3. The measured field map on-resonance (**a**) and 120 Hz off-resonance (**b**), and their difference (**c**).

CONCLUSION

Simulations indicate that the relationship between B_1, B_1^+, and B_1^- becomes complex at higher field strengths. Different RF pulses have different affects on the transmit field distribution and the corresponding RF calibration factors. Off-resonance conditions do not alter the RF calibration factors, but change the distribution of the RF transmit field.

REFERENCES: 1. Stollberger R and Wach P. MRM 1966;35:256
2. Collins et al. MRM 2002;47:1026-8.

ACKNOWLEDGMENTS: Special thanks for support from NIH, NS38467, EB00473, and EB00454